



Biological As(III) Oxidation Coupled with As(V) Interception by Fibrous Anion Exchange Material FFA-1

Junfeng Wan, Rattanak Hai, Yucong Zhang, Lihui Cui, Xiaoying Guo, Fabienne Battaglia-Brunet, Véronique Deluchat, Siguo Yuan, Jiajia Huang, Yan Wang

► To cite this version:

Junfeng Wan, Rattanak Hai, Yucong Zhang, Lihui Cui, Xiaoying Guo, et al.. Biological As(III) Oxidation Coupled with As(V) Interception by Fibrous Anion Exchange Material FFA-1. *Water*, 2022, 14 (6), pp.856. 10.3390/w14060856 . hal-03660088

HAL Id: hal-03660088

<https://brgm.hal.science/hal-03660088>

Submitted on 5 May 2022

HAL is a multi-disciplinary open access archive for the deposit and dissemination of scientific research documents, whether they are published or not. The documents may come from teaching and research institutions in France or abroad, or from public or private research centers.

L'archive ouverte pluridisciplinaire **HAL**, est destinée au dépôt et à la diffusion de documents scientifiques de niveau recherche, publiés ou non, émanant des établissements d'enseignement et de recherche français ou étrangers, des laboratoires publics ou privés.



Distributed under a Creative Commons Attribution 4.0 International License

Article

Biological As(III) Oxidation Coupled with As(V) Interception by Fibrous Anion Exchange Material FFA-1

Junfeng Wan ^{1,2,*}, Rattanak Hai ¹, Yucong Zhang ¹, Lihui Cui ¹, Xiaoying Guo ^{1,2}, Fabienne Battaglia-Brunet ^{3,*}, Véronique Deluchat ⁴, Siguo Yuan ⁵, Jiajia Huang ⁵ and Yan Wang ^{1,2}

¹ School of Ecology and Environment, Zhengzhou University, Zhengzhou 450001, China; haidaxing2018@gmail.com (R.H.); zyc2016_2022@163.com (Y.Z.); 18250197077@163.com (L.C.); xyguo@zzu.edu.cn (X.G.); wangyan371@zzu.edu.cn (Y.W.)

² Henan International Joint Laboratory of Environment and Resources, Zhengzhou 450001, China

³ BRGM—Bureau de Recherches Géologiques et Minières, 45060 Orleans, France

⁴ GRESE—Groupement de Recherche Eau, Sol, Environnement—EA 4330, Université de Limoges, 87060 Limoges, France; veronique.deluchat@unilim.fr

⁵ School of Chemical Engineering, Zhengzhou University, Zhengzhou 450001, China; yuansiguo2005@zzu.edu.cn (S.Y.); huangjiajia@zzu.edu.cn (J.H.)

* Correspondence: wanjunfeng@zzu.edu.cn (J.W.); f.battaglia@brgm.fr (F.B.-B.)

Abstract: A combined process, including As(III) oxidation and As removal by the fibrous anion exchange material FFA-1, was established to treat arsenite ([As(III)] = 10 mg L⁻¹)-polluted groundwater. Both fixed-bed reactors (R1 and R2) were separately filled with pozzolana and FFA-1. After 72 h of inoculation and 10 days of operation, As(III) oxidation efficiency reached around 100% and the total As in the effluent was below 10 µg L⁻¹ for over 100 days. Then, the combined system was stopped and a desorption experiment on the FFA-1 collected from R2 was carried out. The results revealed that the As trapped by the FFA-1 was distributed linearly along the axial length of R2, and the maximum capacity for removal of the FFA-1 from R2 was about 28 mg As g⁻¹ FFA-1. Moreover, the anions' competing test showed that they were preferentially sequestered by the FFA-1 according to the following order: SO₄²⁻ > PO₄³⁻ ≈ AsO₄³⁻ > NO₃⁻ at neutral pH. Furthermore, the microorganisms attached to the FFA-1, including some arsenite-oxidizing microorganisms (AsOBs), could be a beneficial complement to the As(III) oxidation and, thus, the total As removal. At the same time, the regeneration test proved that the As(V) interception capacity of FFA-1 was barely affected by the presence of biofilm. Additionally, the calculated operating cost showed that this combined process has great potential for the remediation of As-polluted groundwater.

Keywords: arsenite oxidation; arsenate interception; anion exchange fiber; interfering anions; regeneration



Citation: Wan, J.; Hai, R.; Zhang, Y.; Cui, L.; Guo, X.; Battaglia-Brunet, F.; Deluchat, V.; Yuan, S.; Huang, J.; Wang, Y. Biological As(III) Oxidation Coupled with As(V) Interception by Fibrous Anion Exchange Material FFA-1. *Water* **2022**, *14*, 856. <https://doi.org/10.3390/w14060856>

Academic Editor: Alexandre T. Paulino

Received: 25 December 2021

Accepted: 2 March 2022

Published: 9 March 2022

Publisher's Note: MDPI stays neutral with regard to jurisdictional claims in published maps and institutional affiliations.



Copyright: © 2022 by the authors. Licensee MDPI, Basel, Switzerland. This article is an open access article distributed under the terms and conditions of the Creative Commons Attribution (CC BY) license (<https://creativecommons.org/licenses/by/4.0/>).

1. Introduction

Long-term exposure to arsenic (As) may cause severe diseases, such as cancers of the skin, lung, and bladder [1,2]. Geological research shows that high levels of As, even up to one milligram per liter, exist in groundwater due to the geological background in many countries, such as Bangladesh and India [3,4]. In addition, many organoarsenic compounds (e.g., roxarsone and *p*-arsanilic acid) have been invented and applied in relation to various human activities [5], which possibly leads to wide and serious As pollution of surface water and shallow groundwater [6].

Nowadays, ion exchange technology has been widely used to treat industrial wastewater, owing to high selectivity, low production of by-product, recoverability of valuable metals, and the ability to meet strict discharge specifications [7–10]. However, the applications of commercialized exchange materials are limited due to the relatively low adsorption rate and some strict conditions [11]. Recently, the ion exchange fiber was invented as a

new material with many potential applications in environment management. Compared with conventional ion exchange resins, the fibrous resin had high adsorption rates and an excellent uptake capacity, because of the short transit distance for the ions and the number of functional groups present along the fiber [12]. Generally, the commonly used ion exchange technique was proved to be more efficient to remove arsenate (As(V)) than arsenite (As(III)) [13], because As(V) exists as a charged oxyanion (H_2AsO_4^- and HAsO_4^{2-}) compared with an uncharged molecule (H_3AsO_3^0), which As(III) exists under neutral conditions [14]. At the same time, As(III) and As(V) are the main forms in the environment, while As(III) is generally dominant in As-polluted groundwater due to reductive conditions [15]. Moreover, As(III) is much more toxic and mobile than As(V) in aquatic environments [16–18]. Hence, the oxidation of As(III) should be beneficially applied as a pre-treatment method before the application of the ion exchange technique.

In fact, with the discovery of numerous arsenite-oxidizing bacteria (AsOB), the biological As(III) oxidation was proven to be an eco-friendly alternative to chemical oxidation for the remediation of As(III)-polluted groundwater [19–22]. Thus, a combined process, consisting of biological As(III) oxidation associated with chemical sequestration, is likely to be effective in removing As(III) from polluted wastewater. Wan et al. [23] investigated a coupled process of biological As(III) oxidation and As(V) removal by zero-valent iron. Furthermore, a combined process of anion exchange technology coupled with the biological method was successfully applied in the treatment of perchlorate- and nitrate-contaminated drinking water [24]. Hence, compared with the main conventional As(III) removal technologies, such as adsorption, membrane separation, ion-exchange, and precipitative processes [25], an original combined process, including biological oxidation and chemical removal methods, should be more green and environmentally friendly; thus, it has a great potential in the remediation of As(III)-polluted groundwater.

Herein, a novel anion exchange functional material named FFA-1 was prepared via grafting copolymerization of triethylenetetramine (TETA) in polyacrylonitrile (PAN) fiber. The chloride anion (Cl^-) located on FFA-1 can exchange with other anions in water solutions such as CrO_4^{2-} ; thus, FFA-1 has a high removal capacity for As(V) in groundwater [26]. In this work, biological pre-oxidation followed by As retention in the FFA-1 fiber reactor was investigated to ultimately remove As(III) from synthetic groundwater. This work was focused on: (1) the long-term performance of the combined process; (2) the effect of biological pre-oxidation and of possible coexisting anions, such as SO_4^{2-} and NO_3^- on As removal by the anion exchange FFA-1; and (3) the feasibility of the combined process for the remediation of As-polluted groundwater.

2. Materials and Methods

2.1. Experimental Set-Up

Two fixed-bed reactors (R1 and R2) with a volume of 185 mL were installed, as shown in Figure 1 [27]. R1 was filled with 188 g of pozzolana ($\varnothing = 4 \pm 1$ mm) used as packing materials, while R2 was filled with 50 g of FFA-1 (a fibrous weak-base anion exchange material, Cl^- form, with standard exchange capacity = $5\text{--}6$ mmol g^{-1}) [26]. The FFA-1 was steeped with 0.1 M HCl and washed with deionized water before utilization. The synthetic groundwater was pumped into R1 at a flow rate of 52.5 ± 0.5 mL h^{-1} . The corresponding hydraulic retention time (HRT) of the reactors (R1 and R2) were controlled at 2.1 and 2.3 h, respectively.

2.2. Inoculation and Substrate Composition

The mixed culture, containing enriched AsOB used as the inoculum, was extracted from a lab-scale sequential batch reactor (SBR) [28]. Then, 10 mL of inoculum was mixed with 100 mL of enrichment medium, as described in Battaglia-Brunet et al. [29], in a glass conical flask and supplemented with 10 mg L^{-1} of As(III). This flask was shaken in a reciprocally agitated incubator (25.0 °C, 140 rpm) for 5 days and was circulated in R1 at a

flow rate of 0.92 L h^{-1} for 72 h before the operation. Dissolved oxygen was $6\text{--}8 \text{ mg L}^{-1}$ in the inflow. The composition of synthetic groundwater is described by Michon et al. [30].

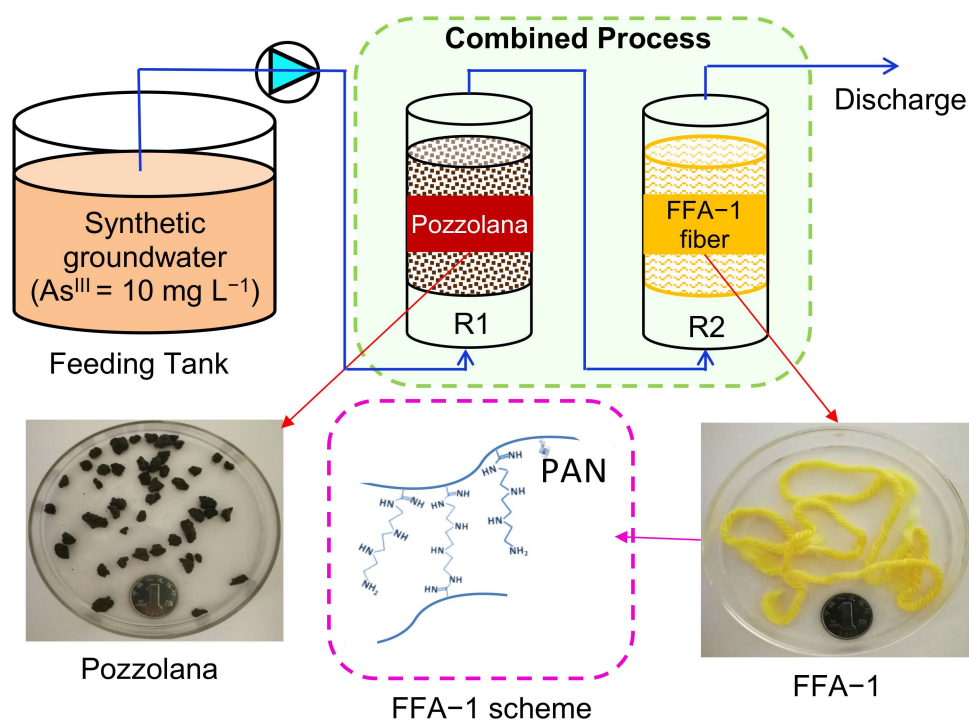


Figure 1. Schematic diagram of the combined system and filling materials.

2.3. FFA-1 Characterization

2.3.1. Micromorphology Observation

The FFA-1 samples which filled R2 were observed with a scanning electron microscope (SEM) (Quanta200) before and after the operation. Prior to SEM imaging, the samples were fixed by immersion in a 2% paraformaldehyde, 2% glutaraldehyde, and $1 \times$ phosphate-buffered saline (PBS) mixed solution overnight at 4°C , with subsequent lyophilization (freeze-drying) [31]. Simultaneously, the elemental composition of the FFA-1 samples was analyzed using an energy dispersive spectrometer (EDS).

2.3.2. Regeneration Test

The reacted FFA-1 was extracted along the axial distance of R2 given the capacity of desorption and re-adsorption of As(V). Prior to the adsorption operation, the As(V)-loaded FFA-1 was eluted with NaOH (0.2 M) solution. Then, the OH^- form of FFA-1 was transferred to the Cl^- form adequately using HCl (0.1 M) solution. Finally, the regenerated FFA-1 (2 g L^{-1}) was tested for its adsorption capacity with water containing $200 \text{ mg As(V) L}^{-1}$ at 140 rpm shaking for 24 h ($\text{pH} = 7.0\text{--}7.5$).

2.3.3. Anion Interference

The selectivity of the FFA-1 (dry weight = 1.0 g) for various anions (AsO_4^{3-} , Cl^- , NO_3^- , PO_4^{3-} , and SO_4^{2-}) was measured in a continuous column experiment (column diameter = 6 mm, height = 10 mm). The influent included arsenate and another possible anion (Cl^- , NO_3^- , PO_4^{3-} , and SO_4^{2-}). The initial concentration of arsenate in the influent was set at 1.25 mmol in order to quickly obtain the breakthrough curve, while chloride (2.5 mmol), nitrate (4.8 mmol), phosphate (1.5 mmol), and sulfate (3.6 mmol) were separately mixed with arsenate in the influent. The initial pH was adjusted at 7.0 ± 0.5 , respectively, with the addition of HNO_3 , H_3PO_4 , H_2SO_4 , and HCl, correspondingly.

2.4. Microbial Diversity Analysis

Microorganism samples were extracted from R1 and R2 at the end of the operation. Microbial DNA of samples was extracted using the E.Z.N.A.[®] Water DNA Kit (Omega Bio-tek, Norcross, GA, USA), according to the manufacturer's protocols. The V4-V5 region of the bacterial 16S *rRNA* gene was amplified by a PCR using primers 338F 5'-barcode-CTCCTACGGGAGGCAGCAG-3' and 806R 5'-GGACTACHVGGGTWTCTAAT-3', where barcode is an eight-base sequence unique to each sample. Amplicons were purified using the AxyPrep DNA Gel Extraction Kit (Axygen Biosciences, Union City, CA, USA) and quantified using QuantiFluor[™]-ST (Promega, Madison, WA, USA). Purified amplicons were pooled in an equimolar and paired-end sequenced (2 × 250) on an Illumina MiSeq platform, according to the standard protocols.

2.5. Analysis Methods

The water samples collected from the feed tank and the outlet of R1 and R2 were immediately filtrated ($\varnothing = 0.45 \mu\text{m}$) and stored at 4 °C before the analysis. The anions' concentrations (Cl^- , SO_4^{2-} , PO_4^{3-} , and NO_3^-) were measured by ion chromatography (Thermo Scientific ICS900). The total As concentration was determined by hydride generation atomic fluorescence spectrometry (HG-AFS) with a quantification limit of $0.5 \mu\text{g L}^{-1}$. As speciation analysis was fulfilled by the high performance liquid chromatograph (HPLC), coupled with HG-AFS with a quantification limit of 0.1 and $0.3 \mu\text{g L}^{-1}$ for As(III) and As(V), respectively. The detailed parameters of HPLC-HG-AFS are described in Yin et al. [5].

2.6. Mass Balance of As

As shown in Equation (1) [23], the incoming As(III) (around 10 mg L^{-1}) resulted in residual As(III) and oxidized As(V) in the effluent of the combined system, and the As was trapped by FFA-1 in R2. Herein, no organic As form was detected in any samples (the limit quantification of monomethylarsonic acid (MMA) and dimethylarsinic acid (DMA) was $1.0 \mu\text{g L}^{-1}$). Hence, the As removal efficiency (η) for the combined system was calculated, as shown by Equation (2) [23].

$$\text{Total As}_{\text{inlet}}^{\text{III}} = \text{As}_{\text{trapped}} + \text{As}_{\text{outlet}}^{\text{V}} + \text{As}_{\text{outlet}}^{\text{III}} \quad (1)$$

$$\eta (\%) = 100 \times \frac{\Delta \text{As}_{\text{trapped}}}{\text{Total As}_{\text{inlet}}^{\text{III}}} = 100 \times \frac{\text{As}_{\text{inlet}}^{\text{III}} - \text{As}_{\text{outlet}}^{\text{III}} - \text{As}_{\text{outlet}}^{\text{V}}}{\text{As}_{\text{inlet}}^{\text{III}}} \quad (2)$$

where $\text{Total As}_{\text{inlet}}^{\text{III}}$ is the concentration of As(III) in the feeding solution; $\text{As}_{\text{outlet}}^{\text{V}}$ and $\text{As}_{\text{outlet}}^{\text{III}}$ are the concentrations of As(V) and As(III) in the effluent of R2, respectively; and $\text{As}_{\text{trapped}}$ is the concentration of As trapped by the FFA-1 of R2.

The arsenite oxidation efficiency (η) for R1 and for R2 could be, respectively, calculated by Equations (3) and (4), because As(III) and As(V) can be hardly adsorbed by the pozzolana in R1, and almost no As(III) (uncharged form existed as H_3AsO_3^0) could be directly adsorbed by the FFA-1 in a neutral pH environment (seen in Supplementary Figure S1).

$$\text{HR}_1 (\%) = 100 \times \frac{\Delta \text{As}_{\text{oxidized}}^{\text{III}}}{\text{Total As}_{\text{inlet}}^{\text{III}}} \quad 100 \times \frac{\text{As}_{\text{outlet}}^{\text{V}}}{\text{As}_{\text{outlet}}^{\text{III}} + \text{As}_{\text{outlet}}^{\text{V}}} \quad (3)$$

$$\eta_{\text{R2}} (\%) = 100 \times \frac{\Delta \text{As}_{\text{oxidized}}^{\text{III}}}{\text{Total As}_{\text{inlet}}^{\text{III}}} \quad 100 \times \frac{\text{As}_{\text{inlet}}^{\text{III}} - \text{As}_{\text{outlet}}^{\text{III}}}{\text{As}_{\text{inlet}}^{\text{III}}} \quad (4)$$

where $\text{As}_{\text{inlet}}^{\text{V}}$ and $\text{As}_{\text{inlet}}^{\text{III}}$ are the concentrations of As(V) and As(III) in the influent, respectively; and $\text{As}_{\text{outlet}}^{\text{V}}$ and $\text{As}_{\text{outlet}}^{\text{III}}$ are the concentrations of As(V) and As(III) in the effluent, respectively.

3. Results

3.1. Performance of Combined System

The combined system operated continuously over 130 days. As shown in Figure 2, the total As in the outlet of R1 fluctuated around 10 mg L^{-1} , which was equal to the influent As(III). On the contrary, the concentration of total As in the effluent of R2 rapidly decreased in one week, then remained below $10 \mu\text{g L}^{-1}$, which meets the standard for drinking water quality suggested by World Health Organization (WHO). Moreover, the removal efficiency (η) of the combined system was almost 100% over 100 days, suggesting that an efficient and stable removal of As(III) was realized by the combined system. After about 130 days of operation, the combined system was stopped while at least 1100 mg As was trapped.

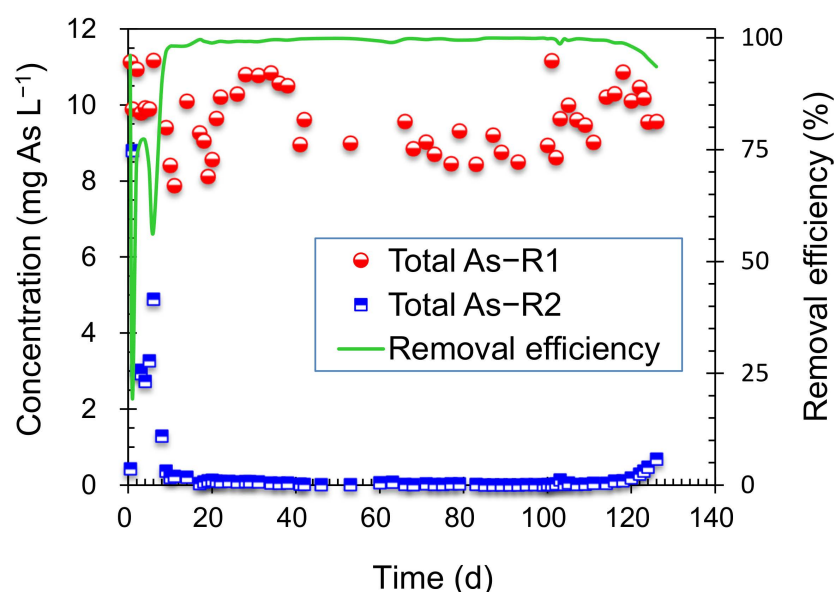


Figure 2. Total As removal by the combined system.

3.2. Arsenite Oxidation in the Combined System

As shown in Figure 3a, after 9 days of microorganism adaption, a large proportion of As(III) was oxidized to As(V) in R1, and then the oxidized As(V) was readily trapped by the FFA-1 in R2. However, the arsenite oxidation efficiency (η) fluctuated between day 53 and day 81, and between day 102 and day 107, because of discontinuous feeding, while the As(III) oxidation efficiency (η) in R2 was higher than 95% at these two above-mentioned phases, according to Equation (4). Moreover, considering that As(III) was hardly trapped by the FFA-1, the residual As(III) present in the R1 outlet could be biologically oxidized and ultimately trapped by the FFA-1 in R2. The performance results of the combined system demonstrated that As(III) and As(V) in the effluent of R2 always remained at a low level ($<10 \mu\text{g L}^{-1}$). In this case, as shown in Figure 3b, although it was difficult to calculate the As(III) oxidation efficiency (η) in R2, the occurrence of biological As(III) oxidation in R2 played a crucial role on the As removal by FFA-1. Meanwhile, the SEM observation (Figure 4) showed that some bacteria were attached to the surface of FFA-1. These microorganisms could contribute to As oxidation in R2.

3.3. Morphological Evolution of FFA-1

The morphology of FFA-1 was observed before and after the operation. The surface of the raw FFA-1 was flat and smooth (Figure 4a). After 130 days of operation, the FFA-1 located at the bottom of R2 was covered by a lot of rough precipitates and some microorganisms (Figure 4b), while some individual bacilli-form microbes adhered to the FFA-1 located at the top of R2 (Figure 4c). As shown in Table 1, the EDS analysis indicated that the chlorine ion content on the surface of FFA-1 after the pre-treatment with HCl (0.1 M) increased to

9.7%, which means the free amino groups of FFA-1 were translated into chlorine ionic types. Compared with the pre-treatment of FFA-1, the chlorine ion content and the As content on the surface of the reacted FFA-1 were 0.3% and 1.2%, respectively.

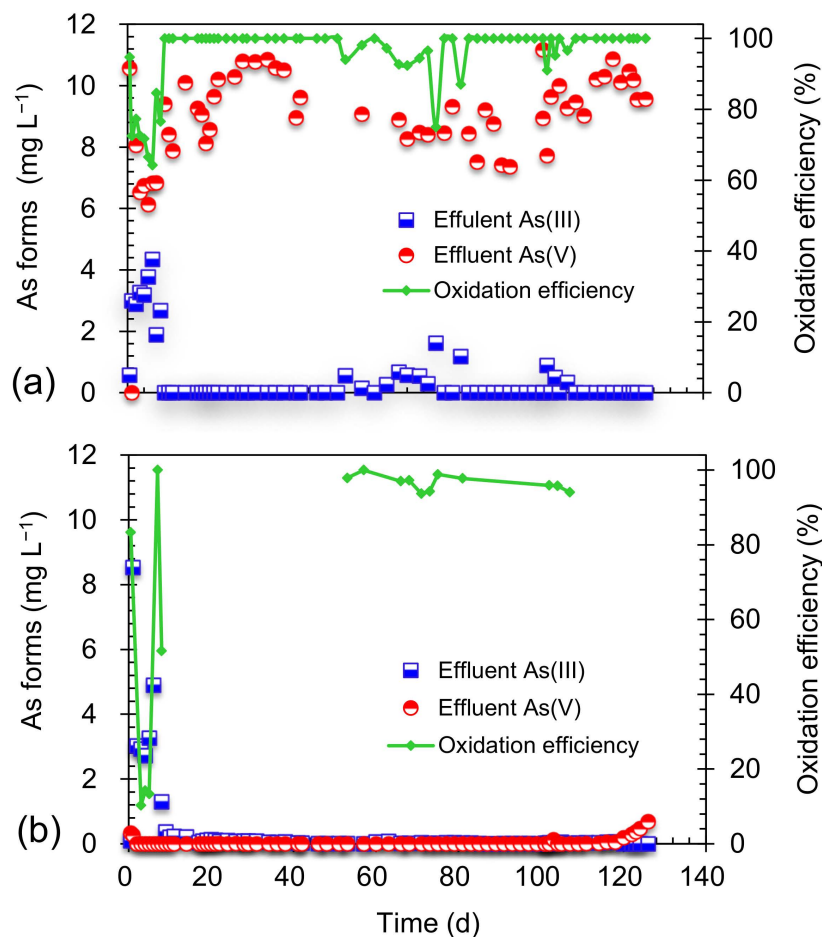


Figure 3. As(III) oxidation in R1 (a) and R2 (b).

3.4. Distribution of As Trapped in R2

On day 130, the total As (the main form was As(V)) in the effluent of R2 was over $10 \mu\text{g L}^{-1}$, the combined system was stopped, and the reacted FFA-1 was carefully extracted from R2. The color of FFA-1 located at the bottom became black. Figure 5a showed that the quantity of As(V) (i.e., adsorbed quantity) desorbed from the reacted FFA-1 at various locations decreased linearly along the axial length of R2. At the same time, a very small amount of desorbed chloride was detected for the reacted FFA-1 at the bottom of R2, which means that the original chloride anion on the surface of FFA-1 was exchanged with other anions such as As(V) and SO_4^{2-} and, thus, almost exhausted (Figure 5b). Figure 4 showed that a higher quantity of material was fixed to the fiber at the bottom of the R2 in comparison with the top of R2. The above-mentioned results revealed that the coexisting anions (e.g., SO_4^{2-} and NO_3^-) could negatively disturb the As removal efficiency by FFA-1 materials. Furthermore, 1g of the collected FFA-1 in R2 maximally adsorbed 28 mg of As, which was much lower than the maximum value (*ca.* 90 mg As per gram FFA-1) in the static batch test with the single As(V) anion solution (seen in Supplementary Figure S1). Meanwhile, the efficiency (i.e., re-adsorption efficiency) of the regenerated FFA-1 at different heights of R2 remained around 90% of the maximum adsorption capacity (Figure 5a,b).

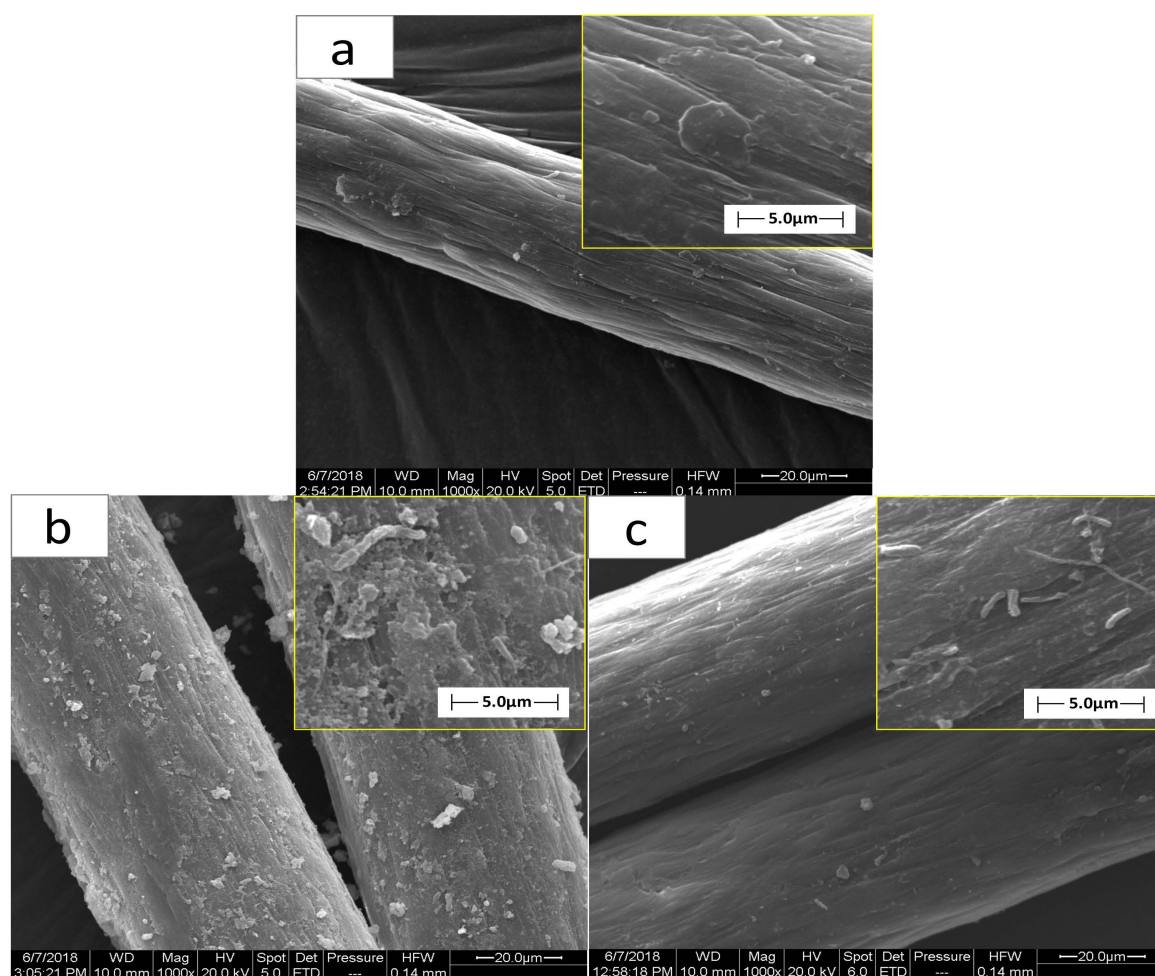


Figure 4. SEM observation of raw FFA-1 (a), reacted FFA-1 at the bottom (b) and the top (c) of R2.

Table 1. Mass percentage of elements on the surface of FFA-1 via EDS analysis.

Element (%)	C	N	O	As	P	S	Cl	Fe
Raw FFA-1	75.4	11.9	12.7	-	-	-	-	-
Pre-treatment FFA-1	63.4	14.6	11.8	-	0.5	-	9.7	-
Reacted FFA-1 in R2	58.6	13.5	18.7	1.2	0.6	5.4	0.3	1.7

In fact, the co-existing anions, such as sulfate (SO_4^{2-}) and nitrate (NO_3^-), present in the synthetic groundwater, could obviously disturb the efficiency of As removal. The distribution of anions trapped by FFA-1 along the axial height of R2 is shown in Figure 5b. These results confirmed that quantities of SO_4^{2-} and NO_3^- were adsorbed in R2, which means the role of competing anions should be considered during the treatment of As-polluted groundwater by the anion exchange resin FFA-1. In this case, phosphate (PO_4^{3-}) in the desorbed solution was hardly detected, probably due to the formation of calcium phosphate that presents a very low solubility. Additionally, the nitrite (NO_2^-) trapped by FFA-1 was detected in R2 and was probably due to denitrification by nitrate-reducing bacteria such as *Thiobacillus* [32], which was documented by the microbial diversity analysis.

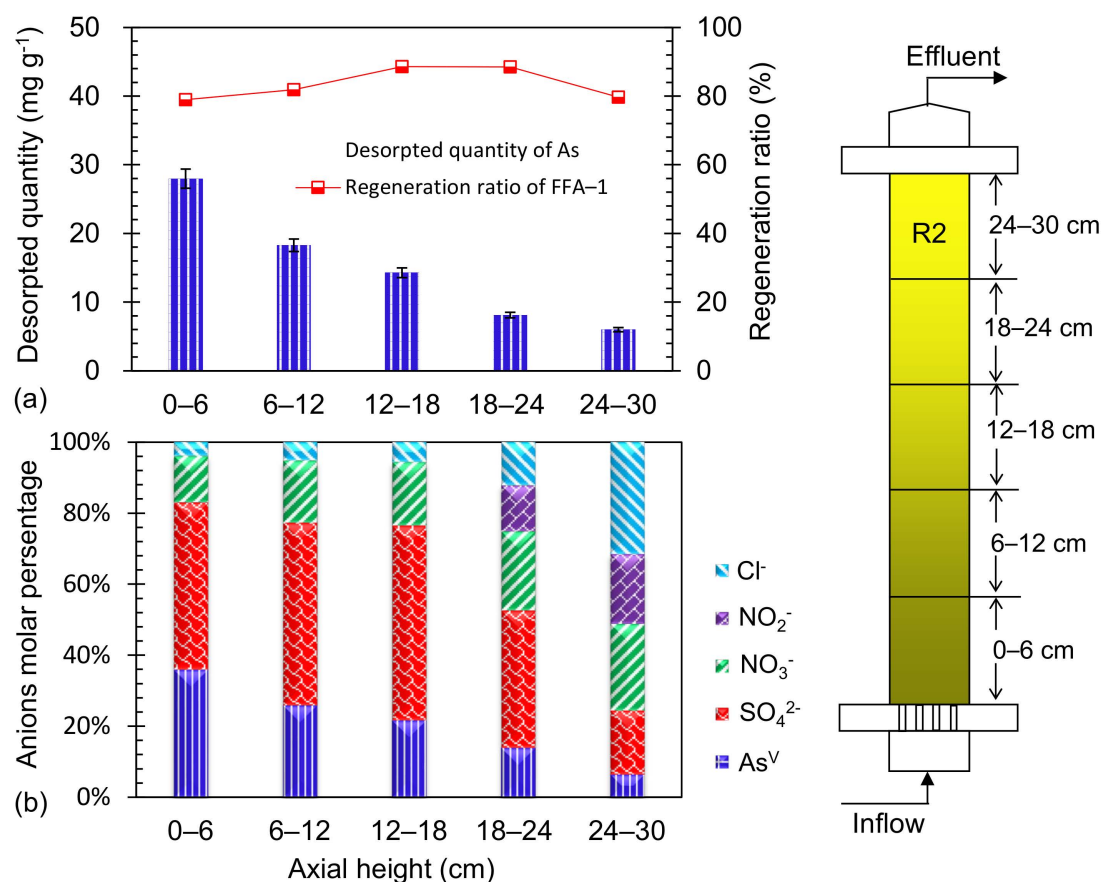


Figure 5. Characterization of FFA-1 at various axial height of R2; quantity of desorbed As and regeneration ratio of FFA-1 (a); distribution of various anions trapped by FFA-1 in R2 (b).

3.5. Effect of Co-Existing Anions on As(V) Removal by FFA-1

In order to further evaluate the effect of possible competing anions (NO_3^- , PO_4^{3-} , and SO_4^{2-}) on arsenate (As(V)) removal by FFA-1, one additional test, fed with a relatively high concentration of potential competing anions, was carried out in the continuous FFA-1 column. The molar substitution rate between chloride ion (Cl^-) and arsenate (As(V)) was about 2.4 in the control test (Figure 6a). When nitrate and arsenate coexisted in the influent, as shown in Figure 6b, nitrate was firstly detected in the effluent and even increased over the initial concentration with the exhaustion of chloride ion from FFA-1, which means that arsenate could not displace nitrate until the chloride was totally depleted. In Figure 6c, phosphate and arsenate appeared in the effluent at the same time, due to their similar structure (Figure 6c). However, arsenate was first detected and strongly desorbed from FFA-1 when sulfate was chosen as the competing anion (Figure 6d). Thus, the order of removal efficiency for anions by FFA-1 is $\text{SO}_4^{2-} > \text{PO}_4^{3-} \approx \text{AsO}_4^{3-} > \text{NO}_3^-$.

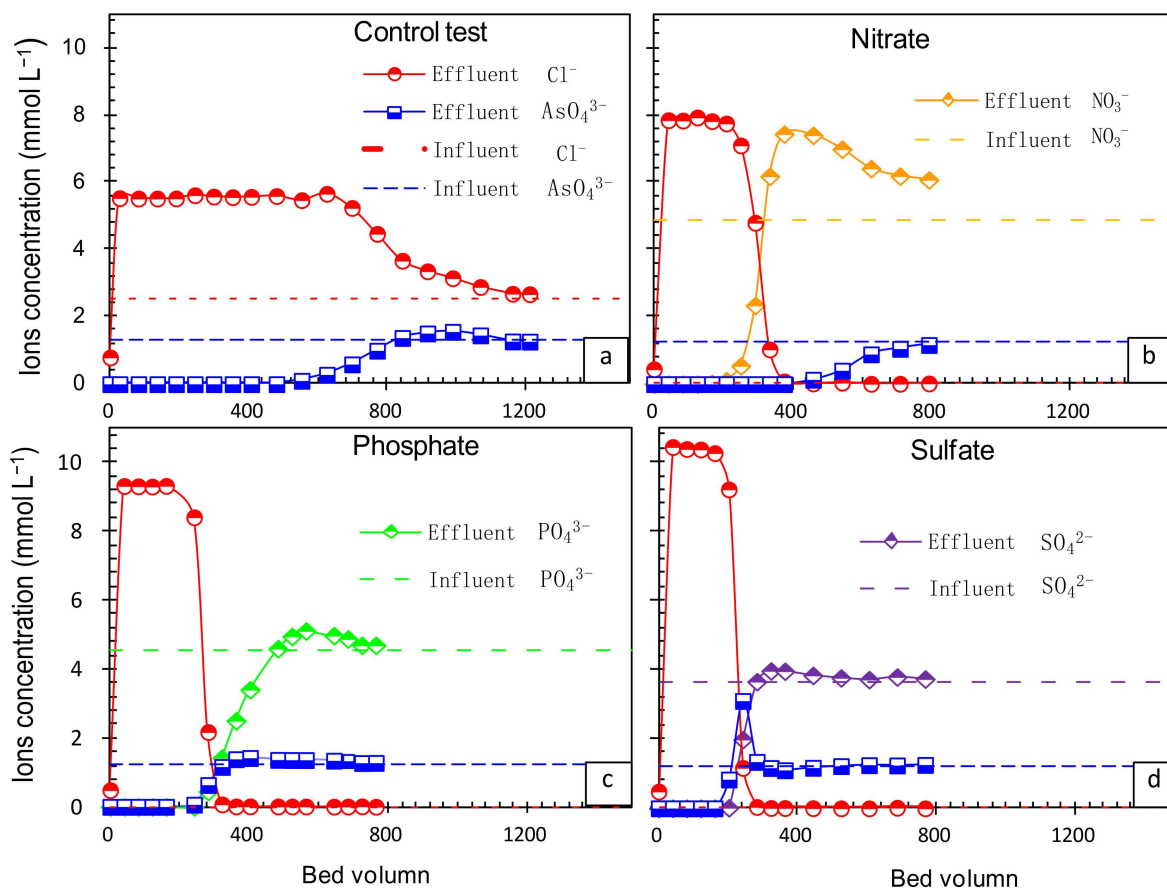


Figure 6. Effect of competing anions (control test (a), nitrate (b), phosphate (c) and sulfate (d)) on the arsenate removal by FFA-1 fiber in continuous column test.

3.6. Microbial Diversity Analysis

After 130 days operation, as shown in the Venn diagram of operational taxonomic units (OTUs) level (Figure 7a), 244 bacterial species-level OTUs were found in the inoculum, among which only 34 OTUs (12.9%) were found in both reactors (Figure 7a). The evolution of the microbial community should be closely related to the inflow substrates (e.g., the concentration of arsenite) and the operating conditions (e.g., dissolved oxygen and pH). R1 and R2 shared 71 common OTUs, accounting for 33% and 46% of their total OTUs, respectively, although no inoculation was performed for R2. The microbial abundances on the class level (Figure 7b) showed that β - and α -proteobacteria were dominant in R1 and R2, the two groups gathering most of the known AsOBs, as reported previously [33]. *Anaerolineae* in R1 was significantly dropped due to the presence of dissolved oxygen in a relatively high concentration (6–8 mg O₂ L^{−1}) in the inflow. Several bacterial genera identified in our treatment system include As(III)-oxidizing strains, i.e., *Pseudomonas*, *Bosea*, *Xanthobacter*, and *Mesorhizobium* (Sultana et al., 2012) [34].

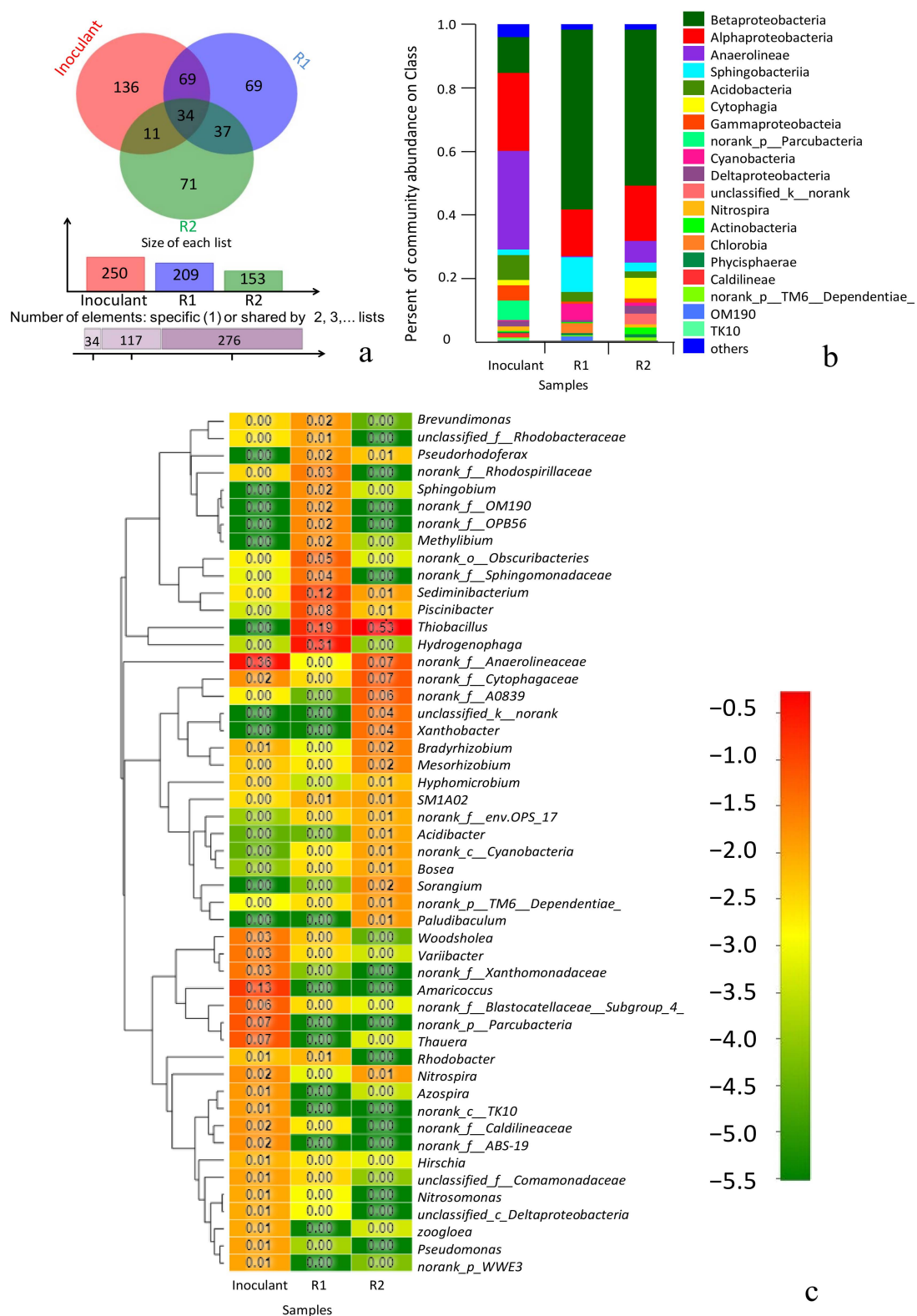


Figure 7. Evaluation of microbial diversity for the inoculum, R1 and R2: Venn diagram of OTUs level (a); histograms of the abundances on class level (b); and hierarchically clustered heatmap graph at the genus level (c).

4. Discussion

4.1. Feasibility of Ion Exchange Technology on As Removal

The data obtained with different ion exchangers for As removal are gathered in Table 2 [13,35–37], showing that 1g of modified polyacrylonitrile fiber could efficiently remove 96.0 mg of As [8], which was similar to the As removal capacity of FFA-1 (Supplementary Figure S1). Herein, their similar fibrous structure could be the key reason for their high As removal capacity [10,11]. Additionally, competing anions such as PO_4^{3-} and F^- could influence the As removal capacity [8,10]. Our study showed that PO_4^{3-} and SO_4^{2-} influence the As removal by FFA-1. However, the regeneration capacity of FFA-1 could exceed 90% even in the presence of bacterial cells attached to its surface.

Table 2. Comparison of As removal capacity via different ion exchangers.

References	Ion Exchanger	Form of Ion Exchanger	As Removal Capacity (mg g^{-1})		Regeneration Ratio (%)	Main Interfering Ions
			As(III)	As(V)		
This study	FFA-1	Fiber	-	82–89	90	PO_4^{3-} , SO_4^{2-}
[10]	Zr-MPR	Bead	-	0.35–0.42 *	-	PO_4^{3-}
[11]	Zr-FCPS	Fiber	-	8.17–9.52	renewable	-
[37]	Vinylbenzyl chloride copolymer coated on a glass fiber	Fiber	-	>5.53	-	-
[8]	Modified polyacrylonitrile fiber	Fiber	-	96.0	-	F^- , PO_4^{3-}
[13]	3-[2-(2-Aminoethylamino)ethylamino]propyl-trimethoxysilanesilica gel	Bead	2	13.2	excellent	-
[36]	Uniselec UR-10	Bead (100–200 mesh)	35.2	39.7	nonrenewable	-
[35]	Iron ^{III} -loaded chelating resin (Fe-LDA)	-	62.9	55.4	renewable	-

* The corresponding unit was mg mL^{-1} .

In order to improve the efficiency of As(V) removal, ion exchange technology was combined with other methods, such as electrodialysis [38] and coagulation [39], to treat wastewater containing As(V). However, As(III) was dominant in As-polluted groundwater due to the reductive condition, while the anion exchangers generally did not efficiently remove As(III), as shown in Table 2. As a consequence, oxidation technology, such as chemical oxidation, was introduced to remove As(III) in ion exchange processes; the literature reveals that most of the previous studies have been performed on As separation by using Fe-loaded resins [40]. Du et al. [41] developed a bifunctional resin-supported nanosized zero-valent iron (NeS-ZVI) composite by combining the oxidation properties of nZVI/ O_2 with the adsorption features of iron oxides and anion-exchange resin NeS. Their results indicated that their maximal adsorption capacity for As(III) was 121 mg g^{-1} .

4.2. Role of Biological Arsenite Oxidation on the Combined Process

Chemical ion exchangers can only remove As(III) from strong alkaline environments [40]. Thus, biological As(III) oxidation could be a cost-effective strategy for the pre-treatment of As removal under neutral conditions. Wan et al. [23] combined biological As(III) oxidation with zero-valent iron to remove concentrated As(III) ($[\text{As(III)}] = 10 \text{ mg L}^{-1}$) from synthetic groundwater. The maximal biological As(III) oxidation rate reached $8.36 \text{ mg h}^{-1} \text{ L}^{-1}$ and about 45% of total As was removed with HRT of 1 h. Moreover, arsenite could be completely biologically oxidized by AsOB, using NO_3 and O_2 as electron acceptors [28]. Based on these results, a novel and integrated As(III) removal process, i.e., biological As(III) oxidation coupled with the fibrous anion exchange technology, was suggested in this work. As shown in Figure 7, the microbial structure evolved in this combined process, with diverse bacteria colonizing R1 then R2. Firstly, over 95% of arsenite was stably oxidized in R1 under low HRT (ca. 2 h). Secondly, the FFA-1 fiber in R2 could

retain the microorganisms from R1 effluent and help to form a biofilm, due to its high specific surface area (Figure 4a).

4.3. Operating Cost

The operating cost of this combined process mainly depends on the consumption of the regenerated chemicals and the loss of FFA-1, regardless of the electricity consumption. Herein, the operating cost can be calculated by Equation (5) [42]:

$$\text{Operating cost (\text{¥}/\text{g As})} = (A + B \times n)/(n + 1) \quad (5)$$

where A (g^{-1} As) is the cost of the first cycle, B (g^{-1} As) is the cost of each regeneration process, n is the number of regenerations, and $(n + 1)$ is the total number of cycles.

Herein, A is a function of the As removal capacity for FFA-1 and the price of FFA-1, while B depends on alkali and acid consumption for the regeneration process; thus, A and B can be obtained from Equations (6) and (7) [42]:

$$A = a_1/a_2 \quad (6)$$

$$B = (C + D)/a_2 \quad (7)$$

where a_1 is the unit price (37 ¥ kg^{-1} FFA-1) and a_2 is the actual exchange capacity (78 g As kg^{-1} FFA-1). C and D are the cost of the alkali cleaning process and the acid pickling process, respectively. Here, the values of C and D are 0.21 and 1.14, respectively (¥ kg^{-1} FFA-1) (the detailed calculation can be seen in the Supplementary Table S2).

As shown in Figure 8, the operating cost per unit volume of groundwater is mainly determined by the initial concentration of As in the groundwater and the number of regeneration cycles, without the consideration of competition from interfering ions. It should be pointed out that the exchange capacity of FFA-1 would decrease with its wear after long-term operation [26], although the effect of the biofilm, including AsOB, on the regeneration ratio of FFA-1 could be ignored.

As shown in Figure 8b, assuming that initial As concentration was 0.5 mg L^{-1} , the calculated operation cost could not decrease obviously, even if the cycle number was more than 10. Therefore, the recommended number of cycles should be less than 10 in order to ensure that As in the effluent of the combined process meets the As requirement (i.e., $10 \text{ }\mu\text{g L}^{-1}$). With the increase in the initial As concentration from 1 to 10 mg L^{-1} , the recommended number of cycles could be in the range from 20 to 50. Herein, the presence of interfering ions, such as sulfate and nitrate, in the polluted groundwater was not considered due to the different characters of groundwater quality in various regions. In order to ensure the quality of the effluent, the penetration removal capacity, rather than the saturated adsorption capacity, is used in the calculation. In the future of real engineering, FFA-1 could be regenerated after saturation by using multi-stage reactors in series which could reduce the operating cost.

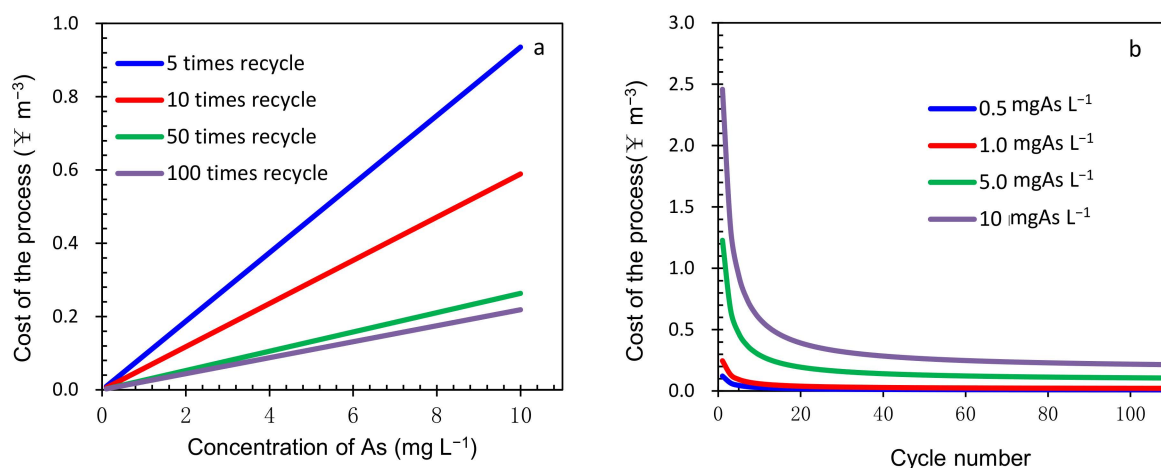


Figure 8. Effect of initial As concentration (a) and cycle time (b) on the operating cost.

5. Conclusions

In this study, the As(III) removal from synthetic groundwater was successfully achieved by using microbial oxidation combined with ion exchange fiber technology. The main conclusions are as follows:

- The combined process can efficiently and reliably remove As(III) from groundwater, achieving effluent total As concentration below $10 \mu\text{g L}^{-1}$ over 130 days;
- Attention should be paid to competing anions (e.g., SO_4^{2-} and NO_3^-) present in the groundwater when the fibrous FFA-1 as an anion exchange material is utilized in the combined process for ultimate As(V) removal;
- This combined process would be economically feasible as an alternative for the remediation of As from polluted groundwater.

Supplementary Materials: The following supporting information can be downloaded at: <https://www.mdpi.com/article/10.3390/w14060856/s1>, Figure S1: Effect of pH (a) and regeneration time (b) on FFA-1 to As(V) removal capacity; Table S1: Composition of the synthetic groundwater; Table S2: Cost analysis table of regeneration process.

Author Contributions: Conceptualization, J.W.; methodology, R.H., X.G. and Y.Z.; software, L.C.; validation, R.H. and Y.Z.; formal analysis, J.H., X.G. and S.Y.; investigation, J.W., F.B.-B. and V.D.; resources, J.W. and S.Y.; data curation, J.H., L.C. and Y.Z.; writing—original draft preparation, J.W., R.H. and Y.Z.; writing—reviewing and Editing, supervision, J.W., F.B.-B., S.Y. and Y.W.; visualization, R.H., J.H., F.B.-B. and V.D.; supervision, J.W. and F.B.-B.; project administration, J.W. and Y.W.; funding acquisition, J.W. All authors have read and agreed to the published version of the manuscript.

Funding: This research received no external funding.

Acknowledgments: The authors thank the National Natural Science Foundation of China (No. 21107100), the Education Department of Henan Province Natural Science Research Program (No. 14A610007), and the Program of Processing and Efficient Utilization of Biomass Resources of Henan Center for outstanding Overseas Scientists (GZS2022007) for the financial support of this study.

Conflicts of Interest: The authors declare no conflict of interest.

References

1. Hughes, M.F. Arsenic toxicity and potential mechanisms of action. *Toxicol. Lett.* **2002**, *133*, 1–16. [CrossRef]
2. Ng, J.C.; Wang, J.; Shraim, A. A global health problem caused by arsenic from natural sources. *Chemosphere* **2003**, *52*, 1353–1359. [CrossRef]
3. Li, C.; Li, F.; Wu, Z.; Cheng, J. Effects of landscape heterogeneity on the elevated trace metal concentrations in agricultural soils at multiple scales in the Pearl River Delta, South China. *Environ. Pollut.* **2015**, *206*, 264–274. [CrossRef] [PubMed]
4. Sharma, A.K.; Tjell, J.C.; Sloth, J.J.; Holm, P. Review of arsenic contamination, exposure through water and food and low cost mitigation options for rural areas. *Appl. Geochem.* **2014**, *41*, 11–33. [CrossRef]

5. Yin, Y.; Wan, J.; Li, S.; Li, H.; Dagot, C.; Wang, Y. Transformation of roxarsone in the anoxic–oxic process when treating the livestock wastewater. *Sci. Total Environ.* **2018**, *616–617*, 1235–1241. [\[CrossRef\]](#) [\[PubMed\]](#)
6. Molinari, R.; Argurio, P. Arsenic removal from water by coupling photocatalysis and complexation-ultrafiltration processes: A preliminary study. *Water Res.* **2017**, *109*, 327–336. [\[CrossRef\]](#)
7. Ficklin, W.H. Separation of arsenic(III) and arsenic(V) in ground waters by ion-exchange. *Talanta* **1983**, *30*, 371–373. [\[CrossRef\]](#)
8. Liu, R.; Guo, J.; Tang, H. Adsorption of fluoride, phosphate, and arsenate ions on a new type of ion exchange fiber. *J. Colloid Interf. Sci.* **2002**, *248*, 268–274.
9. Kim, J.; Benjamin, M.M.; Kwan, P.; Chang, Y. A novel ion exchange process for As removal. *J. Am. Water Work. Assoc.* **2003**, *95*, 77–85. [\[CrossRef\]](#)
10. Awual, M.R.; El-Safty, S.A.; Jyo, A. Removal of trace arsenic(V) and phosphate from water by a highly selective ligand exchange adsorbent. *J. Environ. Sci.* **2011**, *23*, 1947–1954. [\[CrossRef\]](#)
11. Awual, R.; Shenashen, M.; Yaita, T.; Shiwaku, H.; Jyo, A. Efficient arsenic(V) removal from water by ligand exchange fibrous adsorbent. *Water Res.* **2012**, *46*, 5541–5550. [\[CrossRef\]](#) [\[PubMed\]](#)
12. Awual, R.; Shenashen, M.; Jyo, A.; Shiwaku, H.; Yaita, T. Preparing of novel fibrous ligand exchange adsorbent for rapid column-mode trace phosphate removal from water. *J. Ind. Eng. Chem.* **2013**, *20*, 2840–2847. [\[CrossRef\]](#)
13. Fan, H.-T.; Sun, T.; Xu, H.-B.; Yang, Y.-J.; Tang, Q.; Sun, Y. Removal of arsenic(V) from aqueous solutions using 3-[2-(2-aminoethylamino)ethylamino]propyl-trimethoxysilane functionalized silica gel adsorbent. *Desalination* **2011**, *278*, 238–243. [\[CrossRef\]](#)
14. Manning, B.A.; Fendorf, S.E.; Bostick, B.; Suarez, D.L. Arsenic(III) Oxidation and Arsenic(V) Adsorption Reactions on Synthetic Birnessite. *Environ. Sci. Technol.* **2002**, *36*, 976–981. [\[CrossRef\]](#)
15. Nordstrom, D.K. Worldwide Occurrences of Arsenic in Ground Water. *Science* **2002**, *296*, 2143–2145. [\[CrossRef\]](#) [\[PubMed\]](#)
16. Bissen, M.; Frimmel, F.H. Arsenic—A Review. Part II: Oxidation of Arsenic and its Removal in Water Treatment. *Acta Hydrochim. Hydrobiol.* **2003**, *31*, 97–107. [\[CrossRef\]](#)
17. Cullen, W.R.; Reimer, K.J. Arsenic speciation in the environment. *Chem. Rev.* **1989**, *89*, 713–764. [\[CrossRef\]](#)
18. Jain, C.K.; Ali, I. Arsenic: Occurrence, toxicity and speciation techniques. *Water Res.* **2000**, *34*, 4304–4312. [\[CrossRef\]](#)
19. Li, H.; Zeng, X.C.; He, Z.; Chen, X.; Guoji, E.; Han, Y.; Wang, Y. Long-term performance of rapid oxidation of arsenite in simulated groundwater using a population of arsenite-oxidizing microorganisms in a bioreactor. *Water Res.* **2016**, *101*, 393–401. [\[CrossRef\]](#)
20. Corsini, A.; Zaccheo, P.; Muyzer, G.; Andreoni, V.; Cavalca, L. Arsenic transforming abilities of groundwater bacteria and the combined use of *Aliihoeflea* sp. strain 2WW and goethite in metalloid removal. *J. Hazard. Mater.* **2013**, *269*, 89–97. [\[CrossRef\]](#)
21. Dastidar, A.; Wang, Y.-T. Modeling arsenite oxidation by chemoautotrophic *Thiomonas arsenivorans* strain b6 in a packed-bed bioreactor. *Sci. Total Environ.* **2012**, *432*, 113–121. [\[CrossRef\]](#) [\[PubMed\]](#)
22. Ito, A.; Miura, J.-I.; Ishikawa, N.; Umita, T. Biological oxidation of arsenite in synthetic groundwater using immobilised bacteria. *Water Res.* **2012**, *46*, 4825–4831. [\[CrossRef\]](#) [\[PubMed\]](#)
23. Wan, J.; Klein, J.; Simon, S.; Joulain, C.; Dictor, M.-C.; Deluchat, V.; Dagot, C. As(III) oxidation by *Thiomonas arsenivorans* in up-flow fixed-bed reactors coupled to As sequestration onto zero-valent iron-coated sand. *Water Res.* **2010**, *44*, 5098–5108. [\[CrossRef\]](#)
24. Xiao, Y.; Roberts, D.J.; Zuo, G.; Badruzzaman, M.; Lehman, G.S. Characterization of microbial populations in pilot-scale fluidized-bed reactors treating perchlorate- and nitrate-laden brine. *Water Res.* **2010**, *44*, 4029–4036. [\[CrossRef\]](#)
25. Weerasundara, L.; Ok, Y.-S.; Bundschuh, J. Selective removal of arsenic in water: A critical review. *Environ. Pollut.* **2020**, *268*, 115668. [\[CrossRef\]](#) [\[PubMed\]](#)
26. Dai, L.; Cui, L.; Zhou, D.; Huang, J.; Yuan, S. Resource recovery of Cr(VI) from electroplating wastewater: Laboratory and pilot-scale investigation using fibrous weak anion exchanger. *J. Taiwan Inst. Chem. Eng.* **2015**, *54*, 170–177. [\[CrossRef\]](#)
27. Zhang, Y.; Wan, J.; Wang, Y. Removal of trivalent arsenic in water by ion exchange fiber FFA-1 loaded with AsOB. *Acta Sci. Circumstantiae* **2020**, *40*, 1667–1673.
28. Wang, J.; Wan, J.; Li, H.; Li, H.; Dagot, C.; Wang, Y. Biological arsenite oxidation with nitrate as sole electron acceptor. *Environ. Technol.* **2016**, *38*, 2070–2076. [\[CrossRef\]](#) [\[PubMed\]](#)
29. Battaglia-Brunet, F.; Dictor, M.-C.; Garrido, F.; Crouzet, C.; Morin, D.; DeKeyser, K.; Clarens, M.; Baranger, P. An arsenic(III)-oxidizing bacterial population: Selection, characterization, and performance in reactors. *J. Appl. Microbiol.* **2002**, *93*, 656–667. [\[CrossRef\]](#)
30. Michon, J.; Dagot, C.; Deluchat, V.; Dictor, M.-C.; Battaglia-Brunet, F.; Baudu, M. As(III) biological oxidation by CAsO1 consortium in fixed-bed reactors. *Process Biochem.* **2010**, *45*, 171–178. [\[CrossRef\]](#)
31. Hao, T.; Wei, L.; Lu, H.; Chui, H.; Mackey, H.R.; van Loosdrecht, M.C.; Chen, G. Characterization of sulfate-reducing granular sludge in the SANI((R)) process. *Water Res.* **2013**, *47*, 7042–7052. [\[CrossRef\]](#) [\[PubMed\]](#)
32. Baalsrud, K. Studies on *thiobacillus denitrificans*. *Arch. Microbiol.* **1954**, *20*, 34–62. [\[CrossRef\]](#) [\[PubMed\]](#)
33. Oremland, R.S.; Stolz, J.F. The Ecology of Arsenic. *Science* **2003**, *300*, 939–944. [\[CrossRef\]](#)
34. Sultana, M.; Vogler, S.; Zargar, K.; Schmidt, A.C.; Saltikov, C.; Schlömann, S. New clusters of arsenite oxidase and unusual bacterial groups in enrichments from arsenic-contaminated soil. *Arch. Microbiol.* **2012**, *194*, 623–635. [\[CrossRef\]](#) [\[PubMed\]](#)
35. Matsunaga, H.; Yokoyama, T.; Eldridge, R.J.; Bolto, B.A. Adsorption characteristics of arsenic(III) and arsenic(V) on iron(III)-loaded chelating resin having lysine-N α ,N α -diacetic acid moiety. *React. Funct. Polym.* **1996**, *29*, 167–174. [\[CrossRef\]](#)

36. Yoshida, I.; Ueno, K.; Kobayashi, H. Selective Separation of Arsenic(III) and (V) Ions with Ferric Complex of Chelating Ion-Exchange Resin. *Sep. Sci. Technol.* **1978**, *13*, 173–184. [[CrossRef](#)]
37. Dominguez, L.; Economy, J.; Benak, K.; Mangun, C.L. Anion exchange fibers for arsenate removal derived from a vinylbenzyl chloride precursor. *Polym. Adv. Technol.* **2003**, *14*, 632–637. [[CrossRef](#)]
38. Ortega, A.; Oliva, I.; Contreras, K.E.; González, I.; Cruz-Díaz, M.R.; Rivero, E.P. Arsenic removal from water by hybrid electro-regenerated anion exchange resin/electrodialysis process. *Sep. Purif. Technol.* **2017**, *184*, 319–326. [[CrossRef](#)]
39. Oehmen, A.; Valerio, R.; Llanos, J.; Fradinho, J.; Serra, S.; Reis, M.A.; Crespo, J.G.; Velizarov, S. Arsenic removal from drinking water through a hybrid ion exchange membrane–Coagulation process. *Sep. Purif. Technol.* **2011**, *83*, 137–143. [[CrossRef](#)]
40. Mohanty, D. Conventional as well as Emerging Arsenic Removal Technologies—a Critical Review. *Water, Air, Soil Pollut.* **2017**, *228*, 381. [[CrossRef](#)]
41. Du, Q.; Zhang, S.; Pan, B.; Lv, L.; Zhang, W.; Zhang, Q. Bifunctional resin-ZVI composites for effective removal of arsenite through simultaneous adsorption and oxidation. *Water Res.* **2013**, *47*, 6064–6074. [[CrossRef](#)] [[PubMed](#)]
42. Kumar, P.S.; Korving, L.; van Loosdrecht, M.C.; Witkamp, G.-J. Adsorption as a technology to achieve ultra-low concentrations of phosphate: Research gaps and economic analysis. *Water Res. X* **2019**, *4*, 100029. [[CrossRef](#)] [[PubMed](#)]